http://dx.doi.org/10.5012/bkcs.2013.34.12.3835

Green Synthesis of Platinum Nanoparticles by Electroreduction of a K_2PtCl_6 Solid-State Precursor and Its Electrocatalytic Effects on H_2O_2 Reduction

Kyung Tae Kim, Sung-Ho Jin,† Seung-Cheol Chang, and Deog-Su Park*

*Institute of Bio·Physio Sensor Technology, Pusan National University, Busan 609-735, Korea. *E-mail: dsupark@pusan.ac.kr*
†Department of Chemistry Education, Graduate Department of Frontier Materials Chemistry, and Institute for Plastic Information and Energy Materials, Pusan National University, Busan 609-735, Korea
Received August 21, 2013, Accepted October 10, 2013

A new synthesis route for Pt nanoparticles by direct electrochemical reduction of a solid-state Pt ion precursor (K_2PtCl_6) is demonstrated. Solid K_2PtCl_6-supported polyethyleneimine (PEI) coatings on the surface of glassy carbon electrode were prepared by simple mixing of solid K_2PtCl_6 into a 1.0% PEI solution. The potential cycling or a constant potential in a PBS (pH 7.4) medium were applied to reduce the solid K_2PtCl_6 precursor. The reduction of Pt(IV) began at around −0.2 V and the reduction potential was *ca.* −0.4 V. A steady state current was achieved after 10 potential cycling scans, indicating that continuous formation of Pt nanoparticles by electrochemical reduction occurred for up to 10 cycles. After applying the reduction potential of −0.6 V for 300 s, Pt nanoparticles with diameters ranging from 0.02-0.5 μm were observed, with an even distribution over the entire glassy carbon electrode surface. Characteristics of the Pt nanoparticles, including their performance in electrochemical reduction of H_2O_2 are examined. A distinct reduction peak observed at about −0.20 V was due to the electrocatalytic reduction of H_2O_2 by Pt nanoparticles. From the calibration plot, the linear range for H_2O_2 detection was 0.1-2.0 mM and the detection limit for H_2O_2 was found to be 0.05 mM.

Key Words : Platinum nanoparticles, Pt precursors, Electrodeposition, Hydrogen peroxide, Electrocatalysis

Introduction

Platinum nanoparticles have attracted considerable research interest because of their unique physical and chemical properties, many of which are advantageous in numerous research and industrial applications. Platinum nanoparticles are known to function as excellent catalysts for various chemical, electrochemical, and biochemical reactions; accordingly, effective processes for their fabrication are under intensive study.[1,2] Pt nanoparticles are usually prepared from water-soluble metal salts such as H_2PtCl_6, K_2PtCl_6, K_2PtCl_4, $PtCl_2$, $Pt(NH_3)_4(NO_3)_2$, $Pt(AcAc)_2$, $Pt(NH_3)_4Cl_2$, and $Pt(NH_3)_4(OH)_2$, followed by chemical[3-8] or electrochemical reduction.[9-13] Electrochemical reduction, the operationally simple electrolysis of an aqueous solution containing precursors of Pt(II) or Pt(IV), is regarded as a more straightforward, convenient, and eco-friendly process than chemical reduction; although Pt nanoparticle fabrication by electrochemical synthetic methods has many advantages, a number of drawbacks exist. During the electroreduction process, only a fraction of dissolved Pt ions are reduced at the substrate surface, and the precursor remaining in solution is discarded; consequently, current electrochemical techniques for Pt nanoparticle synthesis in the solution phase are undesirable from an environmental standpoint, and are inefficient in terms of obtained conversion ratios of Pt ions to Pt nanoparticles.

Metal ions incorporation in polymers could be used to increase conversion ratios of Pt ions to Pt nanoparticles. Polymer matrices serve as reducing agent, stabilizing agent and/or supporter through complexation reaction with metal ion. Organic polymer assisted metal nanoparticles fabrication offers a variety of opportunities to control the size, shape, and stability of metal nanoparticles. A number of electrochemical preparations of metal nanoparticles with polymer matrices have been studied including Au, Ag, and Pt nanoparticles.[14-17] But, during incorporation step of metal ion into the polymer, metal ions are presented in aqueous solution. A polyethyleneimine (PEI) is a hydrophilic polymer with primary, secondary and tertiary amino groups with positive charge in neutral aqueous solution. The PEI is widely used as a stabilizer for the fabrication of metal nanoparticles.[18,19]

The direct reduction of an electrode-supported solid-state Pt precursor can allow for a more environmentally friendly synthesis and higher Pt ion conversion ratios for Pt nanoparticle preparation. The solubility of Pt salts in aqueous media and suspension of solid Pt salts on conductive substrates must be considered when performing solid-state Pt nanoparticle fabrication. Unlike most Pt salts, K_2PtCl_6 is slightly soluble in cold water (K_{sp} of $K_2PtCl_6 = 7.48 \times 10^{-6}$)[20] and is therefore suitable as a solid precursor for the electrochemically-mediated preparation of Pt nanoparticles. The electrochemical reduction method using solid K_2PtCl_6 suspension has not been reported before as for our knowledge.

In this work, an electrochemical method for preparing polyethyleneimine (PEI)-supported Pt nanoparticles by suspension of a solid precursor composed of K_2PtCl_6 on a glassy carbon (GC) electrode is described. The physical properties of the prepared Pt nanoparticles, as well as electrochemical behaviour and catalytic properties toward the electroreduction of hydrogen peroxide (H_2O_2) are also presented.

Experimental

Materials. Potassium hexachloropalatinate(IV) (K_2PtCl_6), polyethyleneimine (PEI, MW ~1,300), NaH_2PO_4, Na_2HPO_4 and H_2O_2 were purchased from Aldrich (USA) and used without further purification. All solutions were made by deionized water.

Instruments. Cyclic voltammetry and controlled-potential electrolysis measurements were performed with an IVIUM electrochemical workstation (USA). A conventional three-electrode cell was used with Ag/AgCl (saturated KCl), platinum wire, and a glassy carbon electrodes (GCE, diameter: 3 mm) as reference, counter and working electrodes, respectively. Before each experiment, the GCE was polished by using 0.3 and 0.05 μm alumina powders followed by washing with ethanol and distilled water. Before each electrochemical measurement, nitrogen gas was purged through the solution for 5 minutes to remove dissolved oxygen.

The scanning electron microscopy (SEM) experiment was made on a HITACHI S-4200 (Hitachi, Japan). The X-ray photoelectron spectroscopy (XPS) spectra were acquired with a Theta Probe AR-XPS System (Thermo Fisher Scientific, U.K) spectrometer using a monochromated Al-Kα radiation (1486.6 eV) at KBSI (Busan, S. Korea). All data were acquired at an X-ray power of 100 W and an energy step of 0.1 eV. The C(1s) line (binding energy 284.6 eV) was used as an internal reference for calibrating the spectra.

Electrochemical Preparation of Pt Nanoparticles. Before mixing solid K_2PtCl_6 and polyethyleneimine (PEI) solution, K_2PtCl_6 was ground into a fine powder with mortar. The fine powder of K_2PtCl_6 was directly mixed with an aqueous PEI solution. Solid K_2PtCl_6-supported PEI coatings with different wt/vol ratios of K_2PtCl_6/PEI (0.05, 0.5, and 5.0 wt/vol %) were prepared by simple mixing of solid K_2PtCl_6 into a 1.0% PEI solution. For a K_2PtCl_6/PEI mixture of 0.5 wt/vol %, typically, 0.5 mg of finely ground solid K_2PtCl_6 was added to 100 μL of 1.0% PEI solution with mixing over 10 s. A 2 μL quantity of the prepared K_2PtCl_6/PEI mixture was drop-coated on the GC electrode surface and dried at room temperature for 10 min. After drying, potential cycling or constant potential in a phosphate buffer solution (PBS) was applied to reduce the solid K_2PtCl_6 precursor.

Results and Discussion

Electrochemical Synthesis of Pt Nanoparticles. As summarized in Figure 1, a two-step procedure was employed for the fabrication of Pt nanoparticles *via* the following sequence: electrode surface coating of a solid K_2PtCl_6-suspended polyethyleneimine (PEI; MW 1,300) film, followed by direct electroreduction of solid K_2PtCl_6. The PEI functioned as a nanoparticle precursor (K_2PtCl_6) support on the electrode surface.

For the fabrication of Pt nanoparticles, electroreduction using a solid K_2PtCl_6-coated GC electrode was performed by multiple-scan cyclic voltammetry in 0.1 M PBS (pH 7.4). Figure 2(a) shows the successive cyclic voltammograms

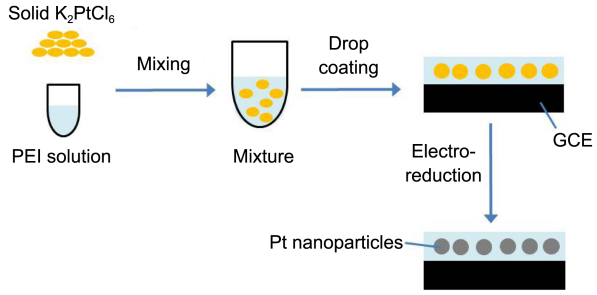

Figure 1. Schematic representation of the Pt nanoparticle fabrication process using solid K_2PtCl_6 *via* electroreduction. PEI; polyethyleneimine, GCE; glassy carbon electrode.

recorded during the electrochemical reduction of a K_2PtCl_6-coated GC electrode (0.5 wt/vol % K_2PtCl_6/PEI) at a scan rate of 100 mV s^{-1} between +1.0 V and 1.0 V *vs.* Ag/AgCl (saturated KCl). Generally, the electrochemical reduction of Pt(IV) was performed under acidic conditions. In this study, in order to maintain the solid state of the Pt ion precursor, a 0.1 M PBS (pH 7.4) medium was used as a supporting electrolyte to decrease the solubility of K_2PtCl_6.

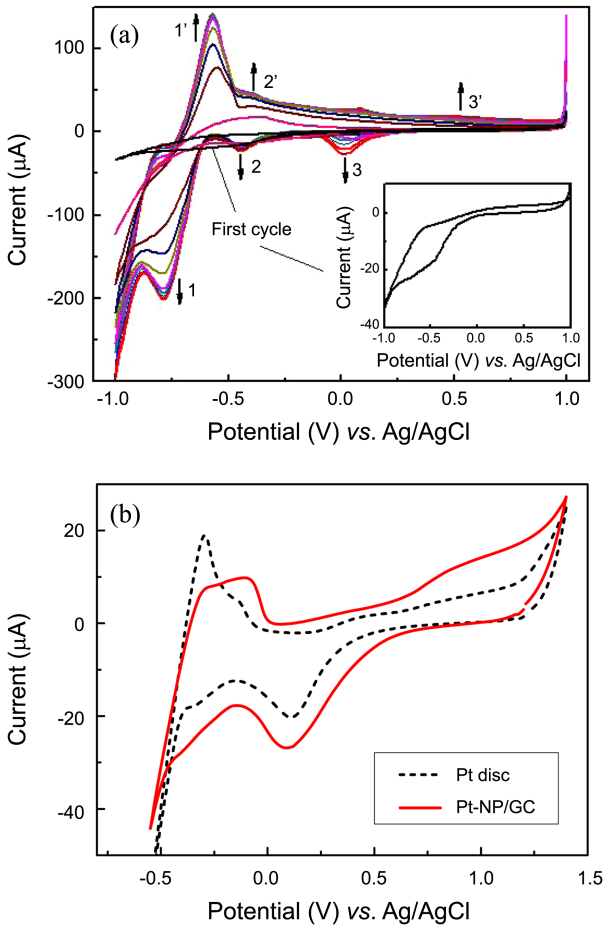

Figure 2. (a) Successive cyclic voltammograms of a 0.5 wt/vol% solid K_2PtCl_6-coated GC electrode in 0.1 M PBS (pH 7.4). Inset shows voltammogram of first potential cycling. (b) Cyclic voltammograms of Pt-NP/GC and conventional Pt disk electrodes in 0.1 M H_2SO_4. Pt loading: 5.0 wt/vol %; scan rate: 100 mV s^{-1}.

During the first scan in the negative direction of potential from 1.0 V to −1.0 V (inset of Figure 2(a)), the reduction of Pt(IV) began at around −0.2 V. No oxidation current can be observed during positive direction of CV scanning, implying that the reduction of Pt(IV) is an irreversible process. In the second potential cycle, the irreversible reduction current of Pt(IV) disappeared, indicating that Pt(IV) was effectively reduced to Pt metal in the first potential cycling.[21] The electrodeposition of Pt from $PtCl_6^{2-}$ involves four electron reduction process including one (Pt(IV) → Pt(0)) or two steps (Pt(IV) → Pt(II) → Pt(0)).[22] On subsequent potential cycling, new redox peaks gradually increase with an increase in the number of cycles, which means that the Pt nanoparticles are growing on the glassy carbon surface during the successive potential scan. A constant current was achieved after 10 potential cycling scans, indicating that no obvious formation of Pt nanoparticles by electrochemical reduction occurred after 10 potential cycles. The resulting voltammograms during potential cycling were similar to those previously reported for electrodeposition of Pt on the carbon electrode in an aqueous Pt(IV) solution.[21-23] The new redox peaks observed during successive potential cycling in Figure 2(a) corresponded to H_2 evolution (1), H_2 adsorption (2), H_2 desorption (2'), oxide reduction (3), and oxide formation (3'), which were in good agreement with earlier reported values for a Pt wire electrode in PBS (pH 7.2).[24] Basically, the electrochemical reduction of Pt(IV) to Pt metal by polymer-immobilized and aqueous Pt ion precursors were the same processes.[17] For the electroreduction of aqueous Pt ion by using cyclic voltammetry in PBS (pH 7.4), a single reduction peak of Pt(IV) to Pt(0) was observed at −0.40 V and formed thin film of Pt metal over the entire GC surface within 10 potential cycling. This indicate that the reduction of Pt(IV) to Pt(0) in aqueous $PtCl_6^{2-}$ precursor is one-step reduction by diffusion process in aqueous Pt precursor. The cyclic voltammogram of PEI-suspended K_2PtCl_6 as shown inset of Figure 2(a), continuous flow of current was observed over −0.40 V indicating that the reduction of Pt(IV) to Pt metal proceeded by multi-step reductions through electroreduction processes of Pt(IV) → Pt(II) → Pt(0).[25] In the PEI-suspended K_2PtCl_6, the Pt ions could not only make a complex with PEI but also adsorbed on the electrode surface. These adsorbed species affect the electroreduction of Pt ions by increasing the concentration of Pt ions on the surface and decreasing the mean free path for lateral diffusion of adsorbed-ions.[17] This means that the Pt nanoparticles are formed effectively in the presence of polymer matrices. The Pt electrode exhibited characteristic electrochemical behaviors in H_2SO_4 solution. Figure 2(b) shows cyclic voltammograms of a conventional Pt disk (dia. = 3 mm) and Pt nanoparticles deposited onto GC electrodes (Pt-NP/GC) in 0.1 M H_2SO_4 solution between −0.5 V~1.3 V. Both the conventional Pt disk and Pt-NP/GC exhibited typical pairs of peaks corresponding to H_2 desorption/adsorption, oxide formation, and oxide reduction at the same potentials. The peak currents of Pt-NP/GC were almost two times greater than that of the Pt disk electrode because of the increased surface area of the Pt nanoparticles.

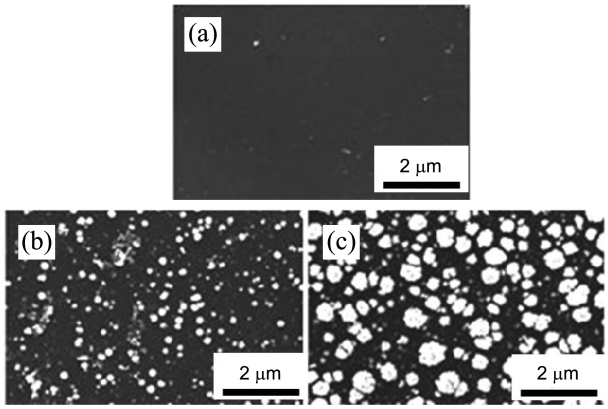

Figure 3. SEM images of Pt nanoparticles electrodeposited on PEI covered glassy carbon electrode under various K_2PtCl_6 concentrations of (a) 0.05, (b) 0.5, and (c) 5.0 wt/vol % of K_2PtCl_6. Applied potential = −0.6 V, deposition time = 300 s.

Characterization of Pt Nanoparticles. Morphological characteristics of the Pt-nanoparticles-deposited GC electrode were studied by scanning electron microscopy (SEM) at different concentrations of K_2PtCl_6, as shown in Figure 3. Pt nanoparticles were electrochemically deposited from the PBS (pH 7.4) solution under a constant potential of −0.6 V, which corresponds to the reduction potential of Pt(IV) as shown in Figure 2(a). When more negative potential than −0.6 V was applied, catalytic production of H_2 was evoked from Pt nanoparticles. Prior to reduction, solid K_2PtCl_6 suspended in the PEI film was observed. After applying the reduction potential for 300 s, Pt nanoparticles were formed with different numbers and diameters at various concentration of K_2PtCl_6. At the K_2PtCl_6 concentration of 0.05 wt/vol %, few number of Pt nanoparticles were formed on the GC surface. When the K_2PtCl_6 concentration was 0.5 wt/vol %, more Pt nanoparticles were formed having diameter of ~0.2 μm. Further increasing the K_2PtCl_6 concentration to 5.0 wt/vol %, Pt nanoparticles with diameters ranging from 0.02-0.8 μm were observed, with an even distribution over the entire GC electrode surface. A greater number of larger particles were obtained from higher concentrations of K_2PtCl_6. Such a behavior is acceptable, because the number of nucleation sites and the particle size increase with the increase in the platinum ion concentration due to the availability of more ions at the electrode surface for reduction.

X-ray photoelectron spectra (XPS) showing the Pt 4f peaks of K_2PtCl_6 powder and the prepared Pt nanoparticles are shown in Figure 4(a) and (b), respectively. Before reduction, the Pt $4f_{7/2}$ and $4f_{5/2}$ peaks of K_2PtCl_6 were presented at 74.7 and 78.1 eV, respectively.[26] After electroreduction under a constant potential of −0.6 V, the Pt $4f_{7/2}$ and Pt $4f_{5/2}$ peaks shifted to 71.3 and 74.6 eV (Figure 4(b)), respectively, which was consistent with that of Pt nanoparticles,[27] providing further evidence that Pt nanoparticles were successfully obtained. The higher XPS peaks than 71.3 and 74.6 eV from convoluted curves at Figure 4(b) could be assigned to PtO and PtO_2 due to Pt oxidation by oxygen or H_2O.[28,29] The

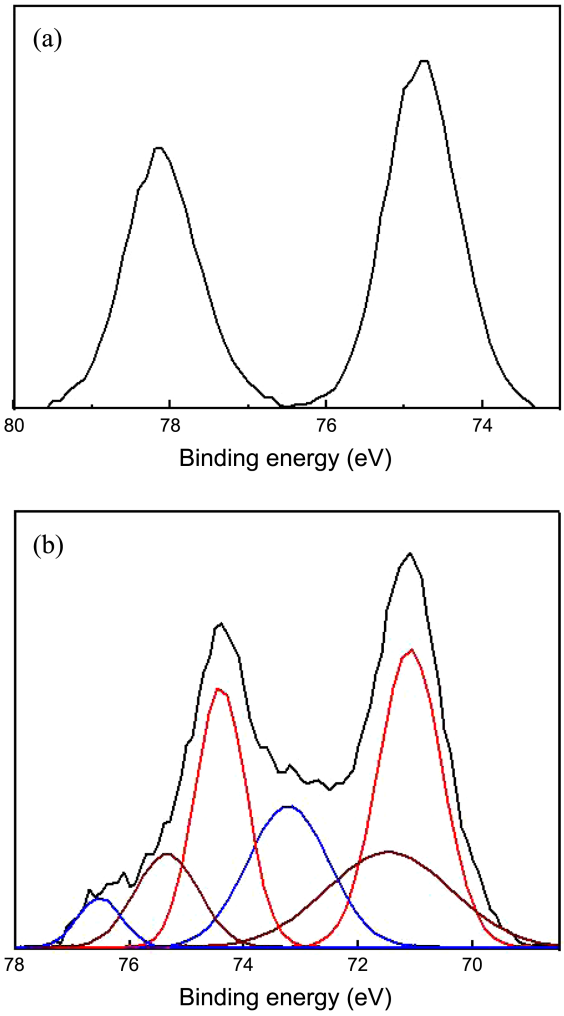

Figure 4. XPS spectra of the Pt 4f for (a) K_2PtCl_6 and (b) Pt nanoparticles.

formation of Pt nanoparticles confirmed by comparing the high-resolu- tion XPS spectra for the Pt ($4f_{7/2}$ and $4f_{5/2}$) region of K_2PtCl_6 powder, K_2PtCl_6 powder suspension in water, K_2PtCl_6 powder suspension in PEI and Pt-NP in PEI, respectively (not shown). From the comparative XPS results, no Pt 4f peaks originated from unreduced Pt ion were observed at those of Pt nanoparticles. So, a solid-state K_2PtCl_6 precursor suspension coated on GC electrode was almost reduced to Pt nanoparticles by electrodeposition within XPS sensitivity (~1%). Except for total electrolysis of Pt ions to Pt metal, only a fraction of dissolved Pt ions are reduced to Pt nanoparticles during electrochemical reduction in solution phase. Therefore the conversion ratio of PEI immobilized Pt precursors was better than that of diffusing Pt ion precursors as shown in XPS results.

Electrocatalytic Reduction of Hydrogen Peroxide. The determination of hydrogen peroxide (H_2O_2) is important in various fields including industrial processes and sensing applications. The electrochemical determination of H_2O_2 has advantages of fast detection, low cost, low detection limit, and high sensitivity. However, the direct electrochemical reduction of H_2O_2 at ordinary solid electrodes is kinetically

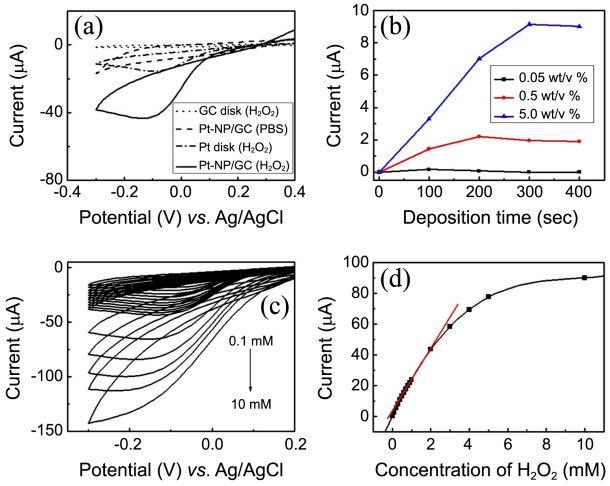

Figure 5. (a) Cyclic voltammograms of bare GC, conventional Pt disk, and 5.0 wt/vol % Pt-NP/GC electrodes for 1.0 mM H_2O_2 (pH 7.4). (b) The effects of K_2PtCl_6 loading and electrodeposition time of K_2PtCl_6 for the electrocatalytic reduction of 1.0 mM H_2O_2 (pH 7.4); deposition potential of K_2PtCl_6 = –0.6 V; scan rate = 50 mV s^{-1}. (c) Cyclic voltammograms for different H_2O_2 concentrations (pH 7.4) using 5.0 wt/vol % Pt-NP/GCE; deposition potential/time of K_2PtCl_6 = –0.6 V/300 s; scan rate = 50 mV s^{-1}. (d) Calibration plot for H_2O_2 determination at 5.0 wt/vol % Pt-NP/GCE. Other conditions are as in Figure 5(c).

slow and requires a large overpotential. The platinum nanoparticles exhibit electrocatalytic behaviour to H_2O_2 and have been widely used for sensing applications. The catalytic effect of the Pt-NP/GC electrode toward H_2O_2 reduction was optimized and showed calibration plot for H_2O_2 determination by cyclic voltammetry.

Figure 5(a) shows cyclic voltammograms recorded using bare GC, conventional Pt disk, and Pt-NP/GC electrodes for a 1.0 mM H_2O_2 solution in 0.1 M PBS (pH 7.4). No reduction peak was observed for H_2O_2 using the bare GC in 0.1 M PBS (dotted line). In the case of Pt-NP/GC electrode in a 0.1 M PBS, small reduction current was observed about 0.1 V corresponding to Pt oxide formation (dashed line). For the Pt-NP/GC electrode in 1.0 mM H_2O_2 solution (solid line), a distinct reduction peak was observed at about −0.20 V because of the electrocatalytic reduction of H_2O_2 by Pt nanoparticles.[30,31] In order to compare the sensitivity of Pt-NP/GC electrode and Pt disc electrode for the determination of H_2O_2, the cyclic voltammogram of conventional Pt disc electrode (dia. = 3 mm) was shown in a solution of 1.0 mM H_2O_2 (dash dotted line). The peak current of Pt-NP/GC was almost three times greater than that of the Pt disk electrode, which could be explained by the increased surface area due to the Pt nanoparticles formation. As expected, no corresponding oxidation peak was observed, since the electrocatalytic reduction process of H_2O_2 is irreversible as shown below:

$$H_2O_2 + 2H^+ + 2e^- \rightarrow 2H_2O \quad (1)$$

At the Pt-NP/GC electrode, it is apparent that the overpotentials are greatly decreased and the reduction currents of

H_2O_2 are also enhanced. The effects of the solid K_2PtCl_6 loading and electroreduction time of solid K_2PtCl_6 were also examined with respect to H_2O_2 reduction (Figure 5(b)) using cyclic voltammetry. The reduction current of H_2O_2 was observed to rise with an increase in K_2PtCl_6 content (0.05, 0.5 and 5.0 wt %) and reduction time. Higher K_2PtCl_6 loadings coupled with extended reduction times resulted in the formation of larger amounts of Pt nanoparticles. Cyclic voltammograms obtained for H_2O_2 detection in PBS (pH 7.4) using a Pt-NP/GC electrode for varying concentrations of H_2O_2 (0.1-10.0 mM) are shown in Figure 5(c). As evidenced by the scans, the reduction current of H_2O_2 was found to increase as the concentration of H_2O_2 increased. As shown by the calibration plot in Figure 5(d), the linear range for H_2O_2 detection in the range 0.1-2.0 mM can be expressed by the following expression:

$$I_p\ (\mu A) = 2.36[C] + 0.84 \quad (2)$$

where, [C] is the concentration (mM) of H_2O_2; the correlation coefficient (R^2) of the linear relations is 0.995 and the detection limit for H_2O_2 is found to be 0.05 mM. The relative standard deviation (RSD) for the determination of H_2O_2 was ± 3.7% for $n = 4$.

Conclusion

In conclusion, we have successfully demonstrated a new synthetic route toward Pt nanoparticles using a solid Pt ion precursor composed of K_2PtCl_6. This novel method for Pt nanoparticle fabrication is electrochemically mediated, utilizing the direct reduction of a solid-state Pt precursor suspension coated on the surface of the GC electrode. Both potential cycling and a constant potential in a PBS (pH 7.4) medium were applied to reduce the solid K_2PtCl_6 precursor. This technique, combining the use of reagents in the solid state with electroreduction techniques, provides an operationally simple method for fabrication of novel nanoparticles for catalytic applications, and offers a more environmentally friendly solution to problems encountered during electroreduction-based procedures in the solution phase.

Acknowledgments. This work was supported by a grant from the National Research Foundation of Korea (NRF) of the Ministry of Education, Science and Technology (MEST) of Korea (No. 2011-0028320).

References

1. Chen, A.; Hindle, P. H. *Chem. Rev.* **2010**, *110*, 3767.
2. Rao, C. R. K.; Trivedi, D. C. *Coord. Chem. Rev.* **2005**, *249*, 613.
3. Şen, F.; Şen, S.; Gökağç, G. *Phys. Chem. Chem. Phys*. **2011**, *13*, 1676.
4. Wang, H. H.; Zhou, Z. Y.; Yuan, Q.; Tian, N.; Sun, S. G. *Chem. Commun.* **2011**, *47*, 3407.
5. Bönnemann, H.; Waldöfner, N.; Haubold, H.-G.; Vad, T. *Chem. Mater.* **2002**, *14*, 1115.
6. Marie, J.; Berthon-Fabry, S.; Chatenet, M.; Chainet, E.; Pirard, R.; Cornet, N.; Achard, P. *J. Appl. Electrochem*. **2007**, *37*, 147.
7. Chen, J.; Herricks, T.; Geissler, M.; Xia, Y. *J. Am. Chem. Soc*. **2004**, *126*, 10854.
8. Qi, Z.; Pickup, P. G. *Chem. Commun*. **1998**, 15.
9. Tiwari, J. N.; Pan, F.-M.; Tiwari, R. N.; Nandi, S. K. *Chem. Commun*. **2008**, 6516.
10. Cui, H. F.; Ye, J.; Zhang, W. D.; Wang, F.; Sheu, F. S. *J. Electroanal. Chem*. **2005**, *577*, 295.
11. Chen, X.; Li, N.; Eckhard, K.; Stoica, L.; Xia, W.; Assmann, J.; Muhler, M.; Schuhmann, W. *Electrochem. Commun*. **2007**, *9*, 1348.
12. Yu, P.; Qian, Q.; Wang, X.; Cheng, H.; Ohsaka, T.; Mao, L. *J. Mater. Chem*. **2010**, *20*, 5820.
13. Park, D. S.; Won, M. S.; Goyal, R. N.; Shim, Y. B. *Sensor. Actuat. B-Chem.* **2012**, *174*, 45.
14. Yin, B.; Ma, H.; Wang, S.; Chen, S. *J. Phys. Chem. B* **2003**, *107*, 8898.
15. Kost, K. M.; Bartak, D. E.; Kazee, B.; Kuwana, T. *Anal. Chem*. **1990**, *62*, 151.
16. Song, J. S.; Kang, C. *Bull. Korean Chem. Soc*. **2007**, *28*, 1683.
17. Song, Y. J.; Oh, J. K.; Park, K. W. *Nanotechnology* **2008**, *19*, 355602.
18. Park, D. K.; Lee, S. J.; Lee, J. H.; Choi, M. Y.; Han, S. W. *Chem. Phys. Lett*. **2010**, *484*, 254.
19. Kuo, P. L.; Chen, W. F.; Huang, H. Y.; Chang, I. C.; Dai, S. A. *J. Phys. Chem. B* **2006**, *110*, 3071.
20. Speight, J. G. *Lange's Handbook of Chemistry*, 16th ed.; McGraw-Hill: Boca Raton, New York, U.S.A., 2005; p 1.338.
21. Ye, J. S.; Ottova, A.; Tien, H. T.; Sheu, F. S. *Bioelectrochemistry* **2003**, *59*, 65.
22. Lu, G.; Zangari, G. *J. Phys. Chem. B* **2005**, *109*, 7998.
23. Stoychev, D.; Papoutsis, A.; Kelaidopoulou, A.; Kokkinidis, G.; Milchev, A. *Mater. Chem. Phys*. **2001**, *72*, 360.
24. Hudak, E. M.; Mortimer, J. T.; Martin, H. B. *J. Neural Eng*. **2010**, *7*, 026005.
25. Zhu, X.; Ding, A. *Int. J. Electrochem. Sci.* **2013**, *8*, 135.
26. Mitchenko, S. A.; Khomutov, E. V.; Shubin, A. A.; Shul'ga, Yu. M. *Theor. Exp. Chem*. **2003**, *39*, 255.
27. Wang, Z.; Shoji, M.; Ogata, H. *Appl. Surf. Sci*. **2012**, *259*, 219.
28. Santiago, D.; Calero, G. G. R.; Palkar, A.; Jimenez, D. B.; Galvan, D. H.; Casillas, G.; Mayoral, A.; Yacamaìn, M. J.; Echegoyen, L.; Cabrera, C. R. *Langmuir* **2012**, *28*, 17202.
29. Santiago, D.; Rodríguez-Calero, G. G.; Rivera, H.; Tryk, D. A.; Scibioh, M. A.; Cabrera, C. R. *J. Electrochem. Soc*. **2010**, *157*, F189.
30. Karam, P.; Halaoui, L. I. *Anal. Chem*. **2008**, *80*, 5441.
31. You, J. M.; Kim, D.; Jeon, S. *Electrochim. Acta* **2012**, *65*, 288.